The growth suppressor $p27^{Kip1}$ protects against diet-induced atherosclerosis

ANTONIO DÍEZ-JUAN AND VICENTE ANDRÉS[1]
Instituto de Biomedicina de Valencia (IBV-CSIC), Spanish Council for Scientific Research, 46010-Valencia, Spain

ABSTRACT **The molecular basis of atherosclerosis is associated with excessive proliferation of vascular cells. Previous studies have suggested an inverse correlation between the expression of the growth suppressor $p27^{Kip1}$ (p27) and cellular proliferation within human atherosclerotic tissue. However, no causal link between diminished p27 expression and atherogenesis has been established. We investigated the effect of p27 inactivation on diet-induced atherogenesis. We find that p27-deficient mice challenged with a high-fat diet for 1 month remain normocholesterolemic and have essentially no visible atheromas. However, when generated in an apolipoprotein E-null genetic background that leads to severe hypercholesterolemia in response to the atherogenic diet, deletion of p27 enhances arterial cell proliferation (~fourfold) and accelerates atherogenesis (~sixfold) compared with apolipoprotein E-deficient mice with an intact p27 gene. Analysis of apolipoprotein E-null mice bearing only one p27 allele inactivated reveals that a moderate decrease in p27 protein expression in the setting of hypercholesterolemia is sufficient to predispose to atherogenesis. Thus, our study establishes a molecular link between decreased p27 protein expression and atherogenesis in hypercholesterolemic animals.—Díez-Juan, A., Andrés, V. The growth suppressor $p27^{Kip1}$ protects against diet-induced atherosclerosis. *FASEB J.* 15, 1989–1995 (2001)**

Key Words: cell cycle · p27 · hypercholesterolemia

TIGHT CONTROL OF cellular proliferation is essential throughout embryonic development and adulthood in higher eukaryotes. Progression through the mammalian cell cycle requires the activation of cyclin-dependent kinases (CDKs) through their association with regulatory subunits called cyclins (1). Different CDK/cyclin holoenzymes are activated at specific phases of the cell cycle. Active CDK/cyclin complexes phosphorylate the retinoblastoma gene product and the related pocket proteins p107 and p130 from mid-G1 to mitosis, which in turn regulate the activity of members of the E2F family of transcription factors (2, 3). Cell proliferation in mammals is negatively regulated by CDK inhibitory proteins (CKIs), which associate with and inhibit the activity of CDK/cyclin holoenzymes (1, 4). CKIs of the CIP/KIP family (p21, p27, and p57) bind to and inactivate a broad range of CDKs, whereas members of the INK4 family (p15, p16, p18, p19) are specific for CDK4- and CDK6-containing holoenzymes.

Coronary artery disease (i. e., atherosclerosis, postangioplasty restenosis, and vein-graft failure) is the leading cause of mortality and morbidity in the Western population (5). The molecular basis of these disorders involves dysregulated growth of vascular smooth muscle cells (VSMCs) and macrophages (6, 7). Accumulating evidence implicates the growth suppressor p27 as an important regulator of the phenotypic response of VSMCs to mitogenic and hypertrophic stimuli, both in vitro and in vivo. First, up-regulation of p27 may limit the growth of VSMCs at late time points after balloon angioplasty (8, 9). Consistent with this possibility, overexpression of p27 efficiently blocked mitogen- and c-fos-dependent induction of cyclin A promoter activity in cultured VSMCs (8, 10), and adenovirus-mediated overexpression of p27 inhibited vascular occlusive lesion formation in balloon-injured arteries (8, 11). Moreover, p27 is hypothesized to serve as a molecular switch that determines whether VSMCs undergo hypertrophic or hyperplastic growth (12, 13). Regarding the role of p27 on hematopoietic cells, it has been suggested that suppression of p27 enhances hematopoietic progenitor cell proliferation and facilitates early development of promyeloid cells into macrophages (14, 15).

Immunohistochemical analysis have suggested an inverse correlation between p27 expression and proliferation of macrophages and VSMCs within human atherosclerotic tissue (9, 16). However, a causal link between p27 and the pathogenesis of atherosclerosis has not been established. In the present study, we investigated the effect of p27 inactivation on diet-induced atherosclerosis. Our study establishes a molecular link between decreased p27 protein expression and atherosclerosis in hypercholesterolemic animals.

MATERIALS AND METHODS

Mice, genotyping, and diets

Mice deficient for apolipoprotein E (apoE) (17) (mixed C57BL/6×129Sv background; gift from J. Osada, Zaragoza,

[1] Correspondence: Instituto de Biomedicina de Valencia (IBV-CSIC), C/Jaime Roig, 11, 46010 Valencia, Spain. E-mail: vandres@ibv.csic.es

Spain) and p27 (18) (C57BL/6 background; gift from M. Serrano, Madrid, Spain) were mated and the double heterozygous F1 offspring were intercrossed. F2 mice were genotyped by PCR analysis and brother-sister mating of p27+/−apoE−/− mice was performed to obtain p27+/+apoE−/−, p27+/−apoE−/−, and p27−/−apoE−/− mice. After weaning, mice were maintained on a low-fat standard diet (2.8% fat, Panlab, Barcelona, Spain). At 2 months of age, mice received for 1 month an atherogenic diet containing 15.8% fat, 1.25% cholesterol, and 0.5% sodium cholate (TD 88051; Harlan/Teklad, Madison, WI). Blood was withdrawn before and after the high-fat diet to measure plasma cholesterol and triglyceride levels using enzymatic procedures (Sigma, St. Louis, MO).

Quantification of atherosclerosis, histomorphometry, and immunohistochemistry

Fat-fed mice were killed and their aortas were fixed in situ with 4% paraformaldehyde. After carefully removing the adventitia, the aorta was excised, fixation was continued overnight, and vessels were opened longitudinally and stained with Oil Red O solution (0.2% in 80% MetOH) (Sigma). Specimens were pinned onto a flat surface and photographed with a Sony DKC-CM30 camera (Tokyo, Japan) mounted on a Zeiss Stemmi 2000-C dissecting scope (Jena, Germany). To determine the extent of atherosclerosis in the aortic arch region (from the aortic root up to ~1.5 mm beyond the left subclavian artery), digital images were analyzed by computer-assisted quantitative morphometry using Sigma Scan Pro v5.0 (Jandel Scientific, San Rafael, CA). For each animal, the area stained with Oil Red O was divided by total investigated area (average ~14 mm^2). Differences in lesion area between males and females were not significant, so data from both sexes were included in these analyses.

The intima-to-media ratio was determined as an independent measure of atheroma formation. In another set of animals, the heart and the proximal aorta were fixed with 100% methanol. Specimens were paraffin-embedded and mounted in a Microm microtome (Heidelberg, Germany). Once the three valve cusps were reached, sections throughout the first ~2 mm of the ascending aorta were discarded. Then, ~25 consecutive sections (5 μm thickness) were taken from two or three regions of the aortic arch separated by ~60 μm. Three cross sections from each region were stained with hematoxylin/eosin. Images were captured with the digital camera mounted on a Zeiss Axiolab stereomicroscope and the area occupied by atherosclerotic lesions (intima) and the area of the media were determined by computer-assisted quantitative morphometry to calculate the intima-to-media ratio. The results for each animal were calculated by averaging all independent values.

Histological examination of methanol fixed cross sections included quantification of cellularity and fibrous cap thickness in the lesions of p27−/−apoE−/− and p27+/+apoE−/− mice. Lesion cellularity was estimated by dividing the number of cells per mm^2 of plaque. The relative fibrous cap thickness was calculated by dividing fibrous cap thickness at the center of the lesion by lesion thickness (19) in 66 fibrous caps from 5 mice of each genotype.

Methanol-fixed cross sections were also analyzed by immunohistochemistry. Proliferation was estimated with anti-PCNA antibodies (1/50, sc-7907, Santa Cruz Biotechnology, Santa Cruz, CA), a biotin/streptavidin-peroxidase detection system (Signet Laboratories, Dedham, MA), and 0.05% (w/v) 3,3′-diaminobenzidine tetrahydrochloride dihydrate substrate (Vector Laboratories; Burlingame, CA). For each mouse, PCNA-positive cells were counted in at least three sections from different regions of the aortic arch and results were averaged. Macrophages were identified using anti-F4/80 antibody (1/10, MCAP497, Serotec, Raleigh, NC) after pretreatment with 0.25% trypsin (3 min, 37°C). Immunocomplexes were detected using biotinylated secondary antibody (sc-2041, Santa Cruz Biotechnology) and alkaline phosphatase-conjugated Streptavidin (Biogenex, San Ramon, CA). VSMCs were identified with alkaline phosphatase-conjugated anti-smooth muscle α-actin (SMα-actin) antibody (1/200, a-5691, Sigma). Alkaline phosphatase activity was detected with Fast Red (Sigma). VSMC content in atherosclerotic lesions was determined morphometrically by dividing the SMα-actin-positive area by total plaque area.

Statistical analysis

Results are reported as mean ± SE. In experiments with two groups, differences were evaluated using a 2-tailed, unpaired *t* test. Analysis involving more than two groups were done using ANOVA and Fisher's post hoc test (Statview, SAS institute, Cary, NC).

Western blot analysis

For each genotype, snap-frozen arteries from three animals were pooled and lysed in ice-cold 50 mM Tris-HCl buffer (pH 7.5) containing 1% Triton X-100, 150 mM NaCl, 1 mM DTT, and protease inhibitor Complete Mini mixture (Roche, Mannheim, Germany) using an Ultraturrax T25 basic (IKA Labortechnik, Staufen, Germany). Western blot analysis was performed as described previously (8) using the following primary antibodies (Santa Cruz Biotechnology): rabbit polyclonal anti-p27 (1/200, sc-776) and mouse monoclonal anti-tubulin (1/200, sc-3035). The relative intensity of protein bands was determined by densitometry.

RESULTS

Effect of p27 inactivation on diet-induced atherosclerosis

We investigated the effect of inactivating p27 on the atherogenic process induced by a high-fat diet. Since as a species the mouse is highly resistant to atherosclerosis (20), we performed our studies in apoE-deficient mice, which develop atherosclerotic lesions resembling those observed in humans (17, 21). By intercrossing mice deficient for p27 and apoE, we generated apoE-null mice bearing various levels of p27 (p27+/+apoE−/−, p27+/−apoE−/−, and p27−/−apoE−/−). Our studies also included p27-null mice with an intact apoE gene (p27−/−apoE+/+). We first examined the plasma triglyceride and cholesterol levels in mice fed either a control diet or a high-fat diet (**Fig. 1**). All mice maintained on control chow exhibited normolipidemia. Likewise, p27−/−apoE+/+ animals challenged with the high-fat diet for 1 month remained normolipidemic. In contrast, fat-fed apoE-deficient mice developed comparable hyperlipidemia regardless of their status for p27. Thus, in agreement with previous studies (17, 21), mice with an intact apoE gene did not display hyperlipidemia when exposed to an atherogenic diet. Moreover, reduction or ablation of p27 did

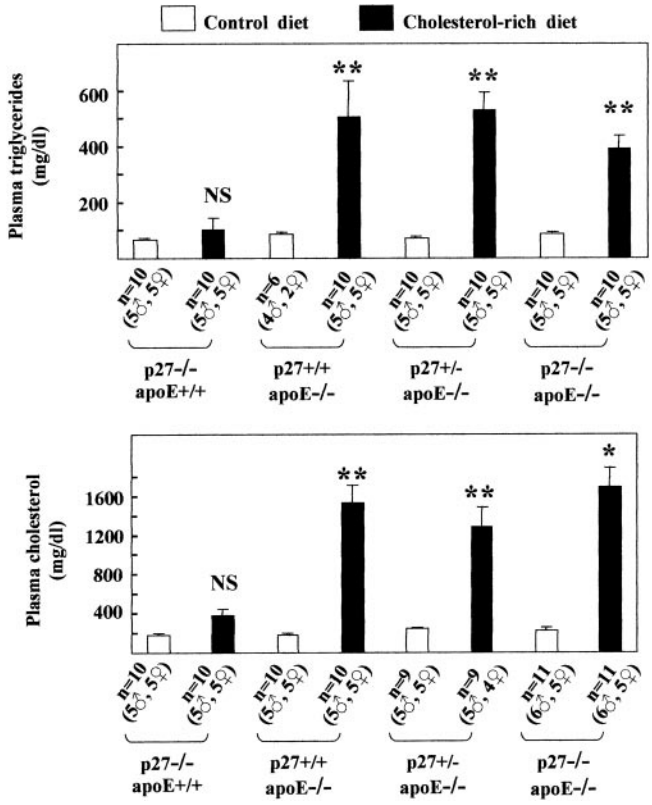

Figure 1. Plasma lipid levels in mice fed control chow or a cholesterol-rich diet. Results represent the mean ± SE of the indicated number of animals. Gender distribution is indicated in parentheses. Open bars: 2-month-old mice fed control chow. Solid bars: 3-month-old mice fed a cholesterol-rich diet for 1 month. Differences in plasma lipid levels among all groups were evaluated using ANOVA and Fisher's PLSD post hoc test. Only comparisons between mice of the same genotype are shown (control vs. cholesterol-rich diet: *$P<0.0003$; **$P<0.0001$); NS, not significant ($P>0.05$). Regardless of their status for p27, all fat-fed apoE-deficient mice developed comparable hyperlipidemia ($P>0.05$).

not affect the hyperlipidemic response normally observed in fat-fed apoE-null mice.

We next analyzed atherogenesis in fat-fed mice by examining whole arteries stained with Oil Red O (**Fig. 2*A***). Based on gross morphological inspection, p27-null mice with intact apoE revealed essentially no visible atheromas. As expected, p27+/+apoE−/− mice developed atherosclerosis in the aorta, which prevailed within the aortic arch. All double nullizygous p27−/− apoE−/− mice revealed augmented atherosclerosis compared with p27+/+apoE−/− mice, and p27 heterozygous mice with inactivated apoE (p27+/−apoE−/−) appeared to have an intermediate phenotype. To rigorously determine the extent of atherosclerosis in these mice, we performed computer-assisted quantitative morphometry of Oil Red O-stained arteries. When compared with p27+/+apoE−/− mice ($n=12$), the area of lesions positive for Oil Red O was enhanced by ~threefold in p27+/−apoE−/− mice ($n=10$, $P<0.002$) and by ~sixfold in p27−/−apoE−/− mice ($n=10$, $P<0.0001$) (Fig. 2*B*). The above findings were confirmed by examination of arterial cross sections stained with hematoxylin/eosin (**Fig. 3*A***). These analyses disclosed an intima-to-media ratio of 0.25 ± 0.02 in p27+/+apoE−/− mice ($n=8$), 0.43 ± 0.06 in p27+/− apoE−/− mice ($n=5$), and 0.96 ± 0.20 in p27−/− apoE−/− mice ($n=8$; $P<0.0015$ vs. p27+/+apoE−/−; $P<0.025$ vs. p27+/−apoE−/−) (Fig. 3*B*). Collectively, these findings indicate that p27 disruption alone is not sufficient to induce atherosclerosis in mice with an intact apoE gene, which remain normolipidemic despite the exposure to a high-fat diet. However, the severity of atherosclerosis in fat-fed apoE-null mice, which develop acute hyperlipidemia, is incrementally exacerbated by inactivation of one or two p27 alleles. As expected, immunoblot analysis revealed the absence of p27 expression in the aorta of p27−/−apoE−/− mice (Fig. 2*C*). Densitometric analysis of two independent blots revealed an average ~42% decrease of p27 protein expression in the aorta of p27+/−apoE−/− compared with p27+/+apoE−/− mice (Fig. 2*C*). Thus, reduction or ablation of p27 expression enhances atherosclerosis in hyperlipidemic mice.

Histological and immunohistochemical characterization of atherosclerotic lesions in p27+/+apoE−/− and p27−/−apoE−/− mice

We then examined the effect of p27 inactivation on the cellular composition of atherosclerotic lesions. Histomorphometric analysis revealed higher cellularity in the lesions of p27−/−apoE−/− mice compared with p27+/+apoE−/− mice (9.7±0.1 cells mm^{-2} vs. 6.6±0.6 cells mm^{-2}, respectively, $n=7$, $P<0.05$) (**Fig. 4*A, C***). In both groups, immunohistochemical analysis using rat monoclonal F4/80 antibody demonstrated the presence of macrophages throughout the intimal lesions (**Fig. 5*C*** and data not shown). We also examined the presence of VSMCs using a mouse monoclonal anti-SMα-actin antibody (Fig. 4*B*). As indicated by the ratio SMα-actin-positive area/total plaque area, VSMCs were more abundant within the lesions of p27−/− apoE−/− mice (0.47±0.05 vs. 0.22±0.08 in p27+/+ apoE−/− mice, $n=7$, $P<0.04$) (Fig. 4*D*). Moreover, relative fibrous cap thickness was greater in p27−/ −apoE−/− mice compared with control animals (0.35±0.02 vs. 0.18±0.02, $n=66$ fibrous caps, $P<0.0001$ (Fig. 4*A, E*). Thus, lesions in the p27−/−apoE−/− mice appeared more advanced, consistent with accelerated atherogenesis in these animals.

We reasoned that enhanced cell proliferation might contribute to augmented atherosclerosis and hypercellularity in the lesions of p27−/−apoE−/− mice. To test this possibility, we performed immunohistochemical analysis using specific antibodies for proliferating cell nuclear antigen (PCNA) as a measure of cell proliferation (22–25). Quantitative analysis revealed that PCNA immunoreactivity in the aortic arch of p27−/−apoE−/− mice was significantly higher than in p27+/+apoE−/− mice, both in the media (fivefold increase, $P<0.0015$) and within atherosclerotic lesions (threefold increase, $P<0.035$) (Fig. 5*A*). To investigate

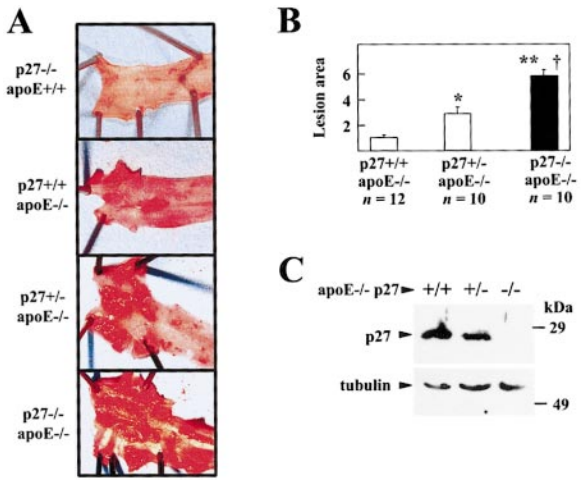

Figure 2. Inactivation of p27 in fat-fed apoE-null mice augments the area of Oil Red O-stained atheromatous plaques. Mice with the indicated genotypes were challenged with a high-fat diet for 1 month. The aorta was dissected out and stained with Oil Red O. *A)* Representative examples of the aortic arch (red regions correspond to atherosclerotic lesions). Atheromatous plaques were essentially negligible in p27−/−apoE+/+ mice. Grossly visible atherosclerotic plaques were evident in all groups of fat-fed apoE-null mice, which predominated within the aortic arch. *B)* Extent of atherosclerosis determined by computer-assisted quantitative morphometry. Results represent the ratio Oil Red O positive area/total area (average total area ~14 mm^2) and are expressed as fold-increase vs. p27+/+apoE−/− mice (=1). Gender distribution for each group was 5 males/7 females (p27+/+apoE−/−), 6 males/4 females (p27+/−apoE−/−), and 5 males/5 females (p27−/−apoE−/−). Statistical analysis: $*P < 0.002$; $**P < 0.0001$, vs. p27+/+apoE−/−; †$P <$ 0.0001 vs. p27+/−apoE−/−. *C)* Immunoblot analysis of cell lysates prepared from the aorta of fat-fed apoE-null mice with the indicated genotype for p27. Primary antibodies were anti-p27 (top) and anti-tubulin (bottom). Relative to p27+/+ apoE−/− mice, aortic p27 expression in p27+/−apoE−/− was 0.58 ± 0.01 (n=2 densitometric analysis normalized by tubulin content).

the identity of proliferating cells, we performed immunohistochemical analysis. By double immunohistochemistry, we found that the majority of PCNA-positive cells in the media of p27+/+apoE−/− and p27−/− apoE−/− mice were also SMα-actin immunoreactive (Fig. 5*B*). In contrast, colocalization of PCNA and SMα-actin was rarely observed within atheromatous plaques (Fig. 5*B*), where PCNA immunoreactivity was seen mainly in macrophage-rich areas (Fig. 5*C*).

DISCUSSION

Ablation of p27 in the mouse leads to enhanced growth, multiorgan hyperplasia, and increased pituitary tumors (18, 26, 27). This phenotype has been attributed to increased cell proliferation, most clearly in tissues that express higher levels of p27. It is accepted that p27 functions as a tumor suppressor gene (28), and p27 also safeguards against excessive cell proliferation during glomerulonephritis and ureteral obstruction (29). Given that excessive proliferation of macrophages and VSMCs underlies the atherogenic process (6), we sought to investigate the effect of p27 inactivation on diet-induced atherosclerosis. These studies were performed in apoE-null mice, a well-characterized animal model of atherosclerosis that recapitulates important features of the human disease (17, 21). Our results demonstrate that a moderate (~42%) reduction in p27 protein expression in the aorta of hyperlipidemic p27+/−apoE−/− mice is sufficient to augment diet-induced atherosclerosis compared with p27+/+ apoE−/− mice, and this phenotype is exacerbated in apoE-null mice lacking both p27 alleles (p27−/− apoE−/−). Fero et al. (30) have demonstrated that p27 is haplo-insufficient for tumor suppression. These authors showed that p27 nullizygous mice are predisposed to tumor formation induced by ionizing radiation or a chemical carcinogen, and p27 heterozygous mice showed intermediate rates of tumorigenesis. Collectively, these studies indicate that a moderate reduction in p27 expression might be sufficient to increase the risk of cancer and atherosclerosis. Indeed, p27

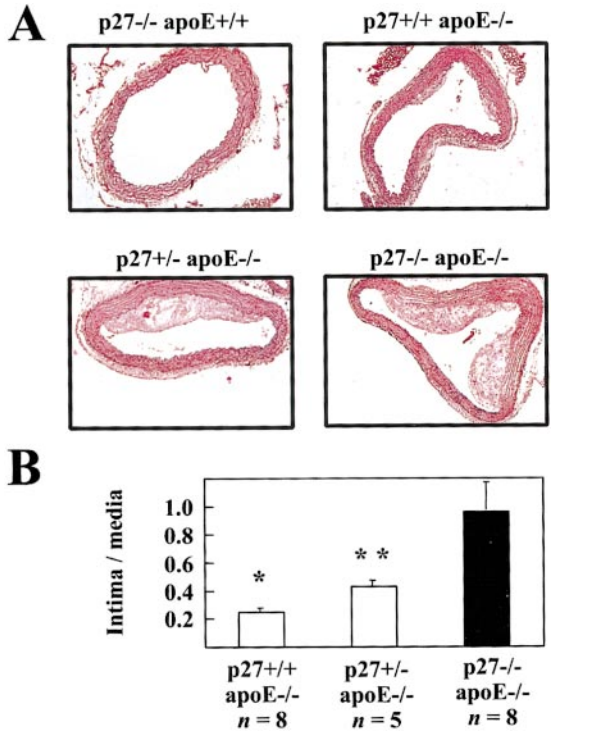

Figure 3. Inactivation of p27 in fat-fed apoE-null mice increases the intima-to-media ratio within the aortic arch. Mice with the indicated genotypes were challenged with a high-fat diet for 1 month. *A)* Representative examples of cross sections from the aortic arch stained with hematoxylin and eosin. Original magnification: 25×. *B)* Quantification of the intima-to-media ratio in cross sections of the aortic arch corroborated the findings with Oil Red-O-stained arteries (see Fig. 2*B*). Gender distribution for each group was 5 males/3 females (p27+/+apoE−/−); 3 males/2 females (p27+/− apoE−/−), and 4 males/4 females (p27−/−apoE−/−). Statistical analysis (vs. p27−/−apoE−/−): $*P < 0.0015$; $**P < 0.025$.

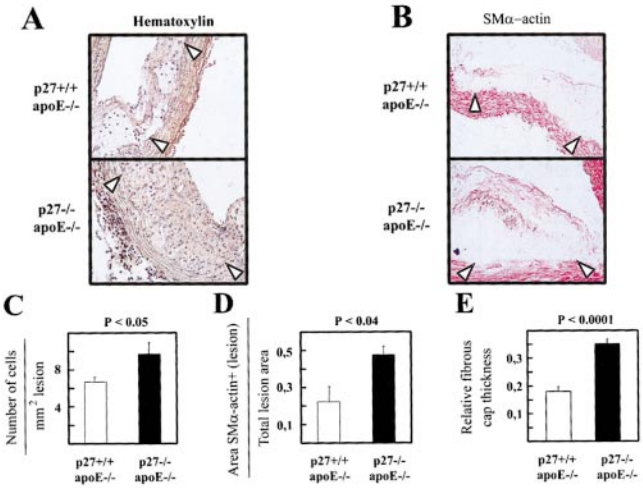

Figure 4. Disruption of p27 enhances lesion cellularity, VSMC content and relative fibrous cap thickness. Cross sections from the aortic arch were stained with hematoxylin (*A*) or immunostained with anti-SMα-actin antibody (*B*). Arrowheads indicate the internal elastic lamina. Original magnification: 100×. Morphometric analysis was performed to quantify lesion cellularity in hematoxylin-stained specimens (*C*) and the area of lesion containing SMα-actin-immunoreactive cells (*D*) (n=7 mice each group). *E)* Relative fibrous cap thickness was calculated by dividing fibrous cap thickness at the center of the lesion by lesion thickness. Results represent the mean ± SE of n = 66 fibrous caps from 5 animals in each group.

expression is frequently down-regulated in human tumors and a reduced level of p27 correlates with poor prognosis (28, 31–33).

Our results suggest that enhanced atherosclerosis in fat-fed p27−/−apoE−/− mice results, at least in part, from increased VSMC and macrophage proliferation. Consistent with our findings, previous studies have shown that p27 is a potent inhibitor of VSMC proliferation (8, 9) and that suppression of p27 expression might promote the proliferation of hematopoietic progenitor cells and their differentiation into macrophages (14, 15). Augmented cell proliferation by disruption of the growth suppressor p53 has been also associated with enhanced atherogenesis in fat-fed apoE-deficient mice (34). Given that the CKI p21 has been detected in human atherosclerotic tissue (9), it will be instructive to test the effect of p21 inactivation on atherogenesis.

Excessive VSMC proliferation is also thought to contribute to restenosis postangioplasty (6, 7). It is hypothesized that induction of endogenous p21 and p27 may limit the hyperplastic growth of VSMCs at late time points after angioplasty in rat and porcine arteries (8, 9, 35). Conversely, p53 inactivation after cytomegalovirus infection may increase the risk of human coronary restenosis (36, 37). Ectopic overexpression of these growth suppressors has proved efficient at limiting neointimal lesion development after experimental angioplasty. These include adenovirus-mediated (8, 11) and rapamycin-dependent (38) overexpression of p27, adenovirus-mediated overexpression of p21 (35, 39, 40), and p53 arterial gene transfer (41). Thus, human studies are warranted to test the efficacy of p27, p21, and p53 overexpression for the inhibition of restenosis after percutaneous interventions.

It is noteworthy that inactivation of either p27 (this study) or p53 (34) by itself is not sufficient to promote atherogenesis in mice challenged with an atherogenic diet for 4–10 wk. Fat-fed p27−/− and p53−/− mice remained normocholesterolemic at the end of the experimental protocol. However, when generated in an apoE-null genetic background that leads to severe hypercholesterolemia in response to the atherogenic diet, ablation of either p27 or p53 accelerated the underlying atherogenic process triggered by hypercholesterolemia. These findings support the notion that excessive vascular cell proliferation is subsidiary to injury to the vessel wall initiated by atherogenic stimuli (i. e., hypercholesterolemia) rather than the cause of this process (6). Another example of a synergistic pathological response involving p27 concerns tumor

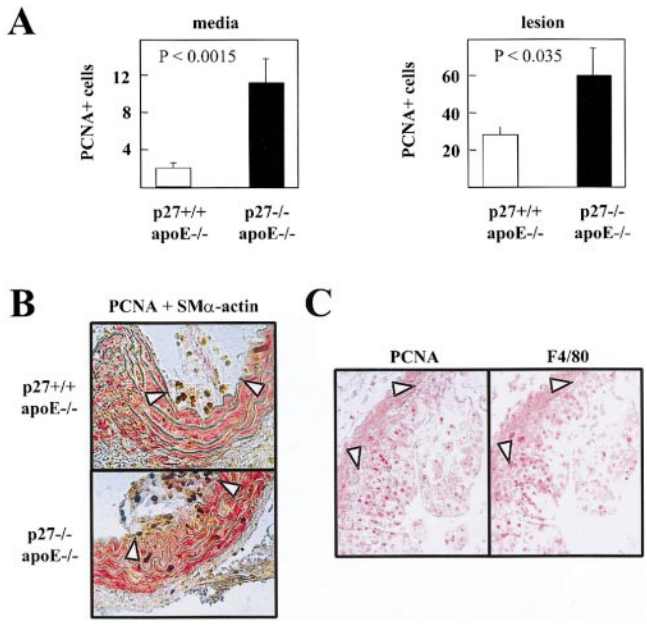

Figure 5. Disruption of p27 enhances arterial cell proliferation in fat-fed mice. Cross sections from the aortic arch were analyzed by immunohistochemistry. *A)* Quantification of the number of PCNA-positive cells in the media and intimal lesions of p27+/+apoE−/− (n=7, 4 males/3 females) and p27−/−apoE−/− (n=6, 3 males/3 females) mice. Results represent the average number of PCNA-immunoreactive cells per cross section. Note that proliferating cells, as indicated by PCNA immunoreactivity, were more abundant in p27−/− apoE−/− mice compared with p27+/+apoE−/− mice, both in the media (P<0.0015) and within lesions (P<0.035). *B)* Double immunostaining using anti-PCNA and anti-SMα-actin antibodies (brown nuclear and red cytoplasmic staining, respectively) revealed abundant proliferating VSMCs within the media. However, colocalization of both antigens was scarce within atheromatous plaques. *C)* Adjacent cross sections of a p27−/−apoE−/− mouse immunostained with anti-PCNA antibody and macrophage-specific anti-F4/80 antibody. Note that PCNA-immunoreactive areas within the lesion correspond generally to macrophage-rich regions. Arrowheads indicate the internal elastic lamina. Original magnification: 200× (*B*) and 100× (*C*).

development. Indeed, spontaneous tumorigenesis in p27-deficient mice appears to be limited to pituitary adenomas (18, 26, 27). However, when challenged with tumorigenic agents (i. e., chemical carcinogens or ionizing radiation), p27-null mice display increased tumor predisposition in multiple tissues (30). These studies suggest that p27 safeguards against the hyperproliferative response triggered by a variety of pathological stimuli.

By the use of genetically modified mice, we have shown that reduced p27 protein expression increases the severity of atherosclerosis induced by hypercholesterolemia. Whether diminished p27 expression may be a common event during atherogenesis remains to be established. Tanner et al. (9) found that p27 protein was abundantly expressed in intimal and medial VSMCs of nonatherosclerotic human coronary arteries. Likewise, p27 expression was commonly observed in regions of coronary atherosclerotic plaques not undergoing proliferation and was absent within proliferating plaque cells. As indicated by double-labeling techniques, the majority of cells expressing p27 in early and advanced human atheromas were VSMCs and macrophages. Ihling et al. (16) also reported p27 immunoreactivity in human atherosclerotic coronary and carotid artery specimens, which localized to nuclei of macrophages, VSMCs, T lymphocytes, and endothelial cells. These authors provided evidence that TGF-β1 present in human atherosclerotic tissue may mediate its growth-suppressive function through p27. Bearing in mind these expression studies and our results demonstrating a causal link between diminished p27 expression and atherogenesis, it is appropriate to consider the role of p27 in an atherosclerotic plaque in influencing both its initial response to mitogenic stimuli and its progression to more advanced stages. Hence, future studies in animal models and human tissue should thoroughly investigate the temporal and spatial pattern of expression of p27 during atherogenesis and elucidate molecular mechanisms underlying the regulation of p27 expression in vascular cells. Such information would find application not only in vascular proliferative diseases, but also in human neoplastic disorders in which tumor progression and patient mortality might be associated with reduced p27 expression (28, 31–33). FJ

We thank J. Roberts, M. Serrano, and J. Osada for providing p27-null and apoE-null mice. We are also grateful to R. Arroyo for technical help, J. Cubells for animal care, and colleagues for critical reading of the manuscript. Work in the laboratory of V.A. is supported in part by grants from the Spanish Dirección General de Educación Superior e Investigación Científica (PM97–0136, 1FD97–1035-C02–02).

REFERENCES

1. Morgan, D. O. (1995) Principles of CDK regulation. *Nature (London)* **374,** 131–134
2. Weinberg, R. A. (1996) E2F and cell proliferation: a world turned upside down. *Cell* **85,** 457–459
3. Lavia, P., and Jansen-Durr, P. (1999) E2F target genes and cell-cycle checkpoint control. *Bioessays* **21,** 221–230
4. Elledge, S. J., and Harper, J. W. (1994) Cdk inhibitors: on the threshold of checkpoints and development. *Curr. Opin. Cell Biol.* **6,** 847–852
5. Tunstall-Pedoe, H., Kuulasmaa, K., Mahonen, M., Tolonen, H., Ruokokoski, E., and Amouyel, P. (1999) Contribution of trends in survival and coronary-event rates to changes in coronary heart disease mortality: 10-year results from 37 WHO MONICA project populations. Monitoring trends and determinants in cardiovascular disease. *Lancet* **353,** 1547–1557
6. Ross, R. (1993) The pathogenesis of atherosclerosis: a perspective for the 1990s. *Nature (London)* **362,** 801–809
7. Libby, P., and Tanaka, H. (1997) The molecular basis of restenosis. *Prog. Cardiovasc. Dis.* **40,** 97–106
8. Chen, D., Krasinski, K., Chen, D., Sylvester, A., Chen, J., Nisen, P. D., and Andrés, V. (1997) Downregulation of cyclin-dependent kinase 2 activity and cyclin A promoter activity in vascular smooth muscle cells by $p27^{Kip1}$, an inhibitor of neointima formation in the rat carotid artery. *J. Clin. Invest.* **99,** 2334–2341
9. Tanner, F. C., Yang, Z.-Y., Duckers, E., Gordon, D., Nabel, G. J., and Nabel, E. G. (1998) Expression of cyclin-dependent kinase inhibitors in vascular disease. *Circ. Res.* **82,** 396–403
10. Sylvester, A. M., Chen, D., Krasinski, K., and Andrés, V. (1998) Role of c-fos and E2F in the induction of cyclin A transcription and vascular smooth muscle cell proliferation. *J. Clin. Invest.* **101,** 940–948
11. Tanner, F. C., Boehm, M., Akyürek, L. M., San, H., Yang, Z.-Y., Tashiro, J., Nabel, G. J., and Nabel, E. G. (2000) Differential effects of the cyclin-dependent kinase inhibitors $p27^{Kip1}$, $p21^{Cip1}$, and $p16^{Ink4}$ on vascular smooth muscle cell proliferation. *Circulation* **101,** 2022–2025
12. Braun-Dullaeus, R. C., Mann, M. J., Ziegler, A., von der Leyen, H. E., and Dzau, V. J. (1999) A novel role for the cyclin-dependent kinase inhibitor $p27^{Kip1}$ in angiotensin II-stimulated vascular smooth muscle cell hypertrophy. *J. Clin. Invest.* **104,** 815–823
13. Servant, M. J., Coulombe, P., Turgeon, B., and Meloche, S. (2000) Differential regulation of $p27^{Kip1}$ expression by mitogenic and hypertrophic factors: involvement of transcriptional and posttranscriptional mechanisms. *J. Cell Biol.* **148,** 543–556
14. Liu, Q., VanHoy, R. W., Zhou, J. H., Dantzer, R., Freund, G. G., and Kelley, K. W. (1999) Elevated cyclin E levels, inactive retinoblastoma protein, and suppression of the $p27^{KIP1}$ inhibitor characterize early development of promyeloid cells into macrophages. *Mol. Cell. Biol.* **19,** 6229–6239
15. Cheng, T., Rodrigues, N., Dombkowski, D., Stier, S., and Scadden, D. T. (2000) Stem cell repopulation efficiency but not pool size is governed by $p27^{kip1}$. *Nat. Med.* **6,** 1235–1240
16. Ihling, C., Technau, K., Gross, V., Schulte-Monting, J., Zeiher, A. M., and Schaefer, H. E. (1999) Concordant upregulation of type II-TGF-beta-receptor, the cyclin-dependent kinases inhibitor $p27^{Kip1}$ and cyclin E in human atherosclerotic tissue: implications for lesion cellularity. *Atherosclerosis* **144,** 7–14
17. Zhang, S. H., Reddick, R. L., Piedrahita, J. A., and Maeda, N. (1992) Spontaneous hypercholesterolemia and arterial lesions in mice lacking apolipoprotein E. *Science* **258,** 468–471
18. Fero, M. L., Rivkin, M., Tasch, M., Porter, P., Carow, C. E., Firpo, E., Plyak, K., Tsai, L.-H., Broudy, V., Perlmutter, R. M., Kaushansky, K., and Roberts, J. M. (1996) A syndrome of multiorgan hyperplasia with features of gigantism, tumorigenesis, and female sterility in $p27^{Kip1}$-deficient mice. *Cell* **85,** 733–744
19. Lutgens, E., Gorelik, L., Daemen, M. J., de Muinck, E. D., Grewal, I. S., Koteliansky, V. E., and Flavell, R. A. (1999) Requirement for CD154 in the progression of atherosclerosis. *Nat. Med.* **5,** 1313–1316
20. Breslow, J. L. (1996) Mouse models of atherosclerosis. *Science* **272,** 685–688
21. Plump, A. S., Smith, J. D., Hayek, T., Aalto-Setälä, K., Walsh, A., Verstuyft, J. G., Rubin, E. M., and Breslow, J. L. (1992) Severe hypercholesterolemia and atherosclerosis in apolipoprotein E-deficient mice created by homologous recombination in ES cells. *Cell* **71,** 343–353
22. Bravo, R., and MacDonald-Bravo, H. (1987) Existence of two populations of cyclin/proliferating cell nuclear antigen during the cell cycle: association with DNA replication sites. *J. Cell Biol.* **105,** 1549–1554

23. Galand, P., and Degraef, C. (1989) Cyclin/PCNA immunostaining as an alternative to tritiated thymidine pulse labelling for marking S phase cells in paraffin sections from animal and human tissues. *Cell Tissue Kinet.* **22,** 383–392
24. Hall, P., Levison, D., Woods, A., Yu, C.-W., Kellock, D., Watkins, J., Barnes, D., Gillet, C., Camplejohn, R., Waseem, N., and Lane, D. (1990) Proliferating cell nuclear antigen (PCNA) immunolocalization in paraffin sections: an index of cell proliferation with evidence of deregulated expression in some neoplasms. *J. Pathol.* **162,** 285–294
25. Kawakita, N., Seki, S., Sakaguchi, S., Yanai, A., Kuroki, T., Mizoguchi, Y., Kobayashi, K., and Monna, T. (1992) Analysis of proliferating hepatocytes using a monoclonal antibody against proliferating cell nuclear antigen/cyclin in embedded tissues from various liver diseases fixed in formaldehyde. *Am. J. Pathol.* **140,** 513–520
26. Nakayama, K., Ishida, N., Shirane, M., Inomata, A., Inoue, T., Shishido, N., Horii, I., Loh, D. Y., and Nakayama, K. (1996) Mice lacking $p27^{Kip1}$ display increased body size, multiple organ hyperplasia, retinal dysplasia, and pituitary tumors. *Cell* **85,** 707–720
27. Kiyokawa, H., Kineman, R. D., Manova-Todovora, K. O., Soares, V. C., Hoffman, E. S., Ono, M., Khanam, D., Hayday, A. C., Frohman, L. A., and Koff, A. (1996) Enhanced growth of mice lacking the cyclin-dependent kinase inhibitor function of $p27^{Kip1}$. *Cell* **85,** 721–732
28. Philipp-Staheli, J., Payne, S. R., and Kemp, C. J. (2001) $p27^{Kip1}$: regulation and function of a haploinsufficient tumor suppressor and its misregulation in cancer. *Exp. Cell Res.* **264,** 148–168
29. Ophascharoensuk, V., Fero, M. L., Hughes, J., Roberts, J. M., and Shankland, S. J. (1998) The cyclin-dependent kinase inhibitor $p27^{Kip1}$ safeguards against inflammatory injury. *Nat. Med.* **4,** 575–580
30. Fero, M. L., Randel, E., Gurley, K. E., Roberts, J. M., and Kemp, C. J. (1998) The murine gene $p27^{Kip1}$ is haplo-insufficient for tumour suppression. *Nature (London)* **396,** 177–180
31. Porter, P. L., Malone, K. E., Heagerty, P. J., Alexander, G. M., Gatti, L. A., Firpo, E. J., Daling, J. R., and Roberts, J. M. (1997) Expression of cell-cycle regulators $p27^{Kip1}$ and cyclin E, alone or in combination, correlate with survival in young breast cancer patients. *Nat. Med.* **3,** 222–225
32. Catzavelos, C., Bhattacharya, N., Ung, Y. C., Wilson, J. A., Roncari, L., Sandhu, C., Shaw, P., Yeger, H., Morava-Protzner, I., Kapusta, L., Franssen, E., Pritchard, K. I., and Slingerland, J. M. (1997) Decreased levels of the cell-cycle inhibitor $p27^{Kip1}$ protein: prognostic implications in primary breast cancer. *Nat. Med.* **3,** 227–230
33. Loda, M., Cukor, B., Tam, S. W., Lavin, P., Fiorentino, M., Draetta, G. F., Jessup, J. M., and Pagano, M. (1997) Increased proteosome-dependent degradation of the cyclin-dependent kinase inhibitor p27 in aggressive colorectal carcinomas. *Nat. Med.* **3,** 231–234
34. Guevara, N. V., Kim, H. S., Antonova, E. I., and Chan, L. (1999) The absence of p53 accelerates atherosclerosis by increasing cell proliferation in vivo. *Nat. Med.* **5(3),** 335–339
35. Yang, Z.-Y., Simari, R. D., Perkins, N. D., San, H., Gordon, D., Nabel, G. J., and Nabel, E. G. (1996) Role of p21 cyclin-dependent kinase inhibitor in limiting intimal cell proliferation in response to arterial injury. *Proc. Natl. Acad. Sci. USA* **93,** 7905–7910
36. Speir, E., Modali, R., and Huang, E.-S. (1994) Potential role of human cytomegalovirus and p53 interaction in coronary restenosis. *Science* **265,** 391–394
37. Zhou, Y. F., Leon, M. B., Waclawiw, M. A., Popma, J. J., Yu, Z. X., Finkel, T., and Epstein, S. E. (1996) Association between prior cytomegalovirus infection and the risk of restenosis after coronary atherectomy. *N. Engl. J. Med.* **335,** 624–630
38. Gallo, R., Padurean, A., Jayaraman, T., Marx, S., Rogue, M., Adelman, S., Chesebro, J., Fallon, J., Fuster, V., Marks, A., and Badimon, J. J. (1999) Inhibition of intimal thickening after balloon angioplasty in porcine coronary arteries by targeting regulators of the cell cycle. *Circulation* **99,** 2164–2170
39. Chang, M. W., Barr, E., Lu, M. M., Barton, K., and Leiden, J. M. (1995) Adenovirus-mediated over-expression of the cyclin/cyclin-dependent kinase inhibitor, p21 inhibits vascular smooth muscle cell proliferation and neointima formation in the rat carotid artery model of balloon angioplasty. *J. Clin. Invest.* **96,** 2260–2268
40. Ueno, H., Masuda, S., SNishio, S., Li, J. J., Yamamoto, H., and Takeshita, A. (1997) Adenovirus-mediated transfer of cyclin-dependent kinase inhibitor p21 suppresses neointimal formation in the balloon-injured rat carotid arteries in vivo. *Ann. N.Y. Acad. Sci.* **811,** 401–411
41. Yonemitsu, Y., Kaneda, Y., Tanaka, S., Nakashima, Y., Komori, K., Sugimachi, K., and Sueishi, K. (1998) Transfer of wild-type p53 gene effectively inhibits vascular smooth muscle cell proliferation in vitro and in vivo. *Circ. Res.* **82,** 147–156

Received for publication February 21, 2001.
Revised for publication May 29, 2001.